PROCEEDINGS of the
23rd International Congress on Acoustics
9 to 13 September 2019 in Aachen, Germany

Acoustic path database for ANC in-ear headphone development

Stefan LIEBICH, Johannes FABRY, Peter JAX, Peter VARY

[1]Institute of Communication Systems, RWTH Aachen University, Germany, {liebich, fabry, jax, vary}@iks.rwth-aachen.de

Abstract

Active noise cancellation (ANC) for headphones is an emerging field with growing interest in consumer applications. Developing such an ANC system involves modeling the system from measurements, designing the algorithms and simulating the performance before building a real-time system. Modeling the system considers the transfer functions between loudspeaker and microphones, called secondary and feedback paths, as well as the relative transfer function between the microphones, called primary path. These paths are modeled with varying degrees of accuracy in the development process: From coarse physical models, e.g., with pure delay; over measured paths under ideal conditions, called nominal; to considering uncertainty due to various operating conditions. However, very few measured paths of ANC headphones publically available. Hence, this publication describes an alongside published database containing two measurement sets of the Bose QC20 in-ear headphone without ANC electronics. The first set contains primary, secondary and feedback paths of 23 subjects measured in an acoustic booth. The second set contains primary paths measured for equally distributed directions on a horizontal plane acquired in a semi-anechoic chamber with a dummy head. The database can be used to consider inter-person differences and direction-of-arrival dependency in algorithm design and simulation.

Keywords: Active Noise Control, Active Noise Cancellation, ANC, Acoustic Paths, Database

1 INTRODUCTION

Real-world audio signal processing problems are usually very complex. They are depending on the acoustic front-end, e.g. a specific headphone design, and often involve time-varying acoustic conditions. Thus, various simplifying steps are made during the development of audio signal processing algorithms. For the development of an ANC system a four step approach, which might be applied recursively, is suggested by Elliott [3]:

1. Simulation by using simplified analytical models
2. Simulation with measured acoustic paths under ideal control conditions, i.e. only nominal paths.
3. Simulation with measured acoustic paths under a variety of operating conditions, i.e. perturbed paths including deviations from nominal path.
4. Implementation of a real-time system and testing under all conditions, to verify predicted behaviour.

The different steps from 1. to 4. involve increasing complexity and they step by step lead to a real-time system. In ANC publications, often very simple and unrealistic system models are used, such as unit delays. They might be adequate for explaining certain behaviours, but are certainly not useful for demonstrating real performance. At the same time very few measurements of actual ANC transmission paths are publically available. This gap is addressed by our publication, which describes a database containing a large number of measurements with a Bose QC20 ANC headphone without ANC electronic, both with human subjects and a dummy head.

The database is named *IKS Paths for Active Noise Cancellation Development And Research* (iks | PANDAR) and available under `http://iks.rwth-aachen.de/PANDAR/`. Before describing the measurement setups, the results and the database structure, a short background in ANC is given in the following section.

2 ANC BACKGROUND

To actively attenuate an acoustic disturbance signal, an ANC system creates a control signal which is emitted by a loudspeaker. This control signal destructively interferes with the disturbance signal. To acquire information

about the disturbance, an ANC headphone typically contains an outer microphone, recording the outer disturbance, and an inner microphone capturing the signals within the ear canal. When using only the outer microphone signal, the system is called a *feedforward* systems [3]. When only the inner microphone is used, the system is called a *feedback* system. Fig. 1a gives an overview of an the underlying signal processing aspects for an in-ear headphone. The illustration shows a combined feedforward-feedback approach. On the acoustic side,

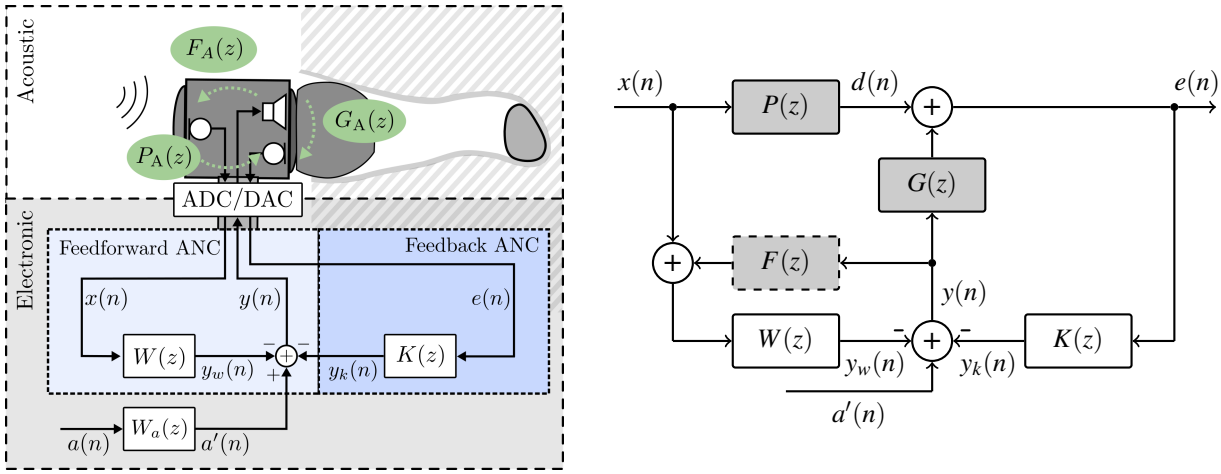

(a) Structure.

(b) Discrete model.

Figure 1. ANC headphones structure and discrete model.

three transmission paths are of interest: the primary path $P(z)$ (outer to inner microphone), the secondary path $G(z)$ (speaker to inner microphone) and the acoustic feedback path $F(z)$ (speaker to outer microphone). Fig. 1a only illustrates the acoustic components of these transmission paths for the sake of readability. The detailed components are outlined in the next section and shown in Fig. 2. On the electronic side, the control signal $y(n)$ is a combination of the feedforward control signal $y_w(n)$ and the feedback control signal $y_k(n)$. $y_w(n)$ is created by filtering the outer disturbance signal $x(n)$, acquired by the outer microphone, with the feedforward filter $W(z)$. $y_k(n)$ is acquired by filtering the error signal $e(n)$, acquired by the inner microphone, with the feedback filter (also known as feedback controller) $K(z)$. A desired audio signal $a(n)$, e.g. a music or a telephone signal, can also be inserted into the control signal. It might require additional prefiltering $W_a(z)$ to account for loudspeaker characteristic and influence of the feedback control. From this, the discrete model in Fig. 1b can be deduced for the filter design. Without loss of generalization we assume $a(n) = 0$. Based on the model, the overall transfer function from $x(n)$ to $e(n)$ is

$$\frac{E(z)}{X(z)} = \frac{P(z) - G(z)W(z)\frac{1}{1+F(z)W(z)}}{1 + G(z)K(z)\frac{1}{1+F(z)W(z)}} \overset{F(z)\approx 0}{\approx} = \frac{P(z) - G(z)W(z)}{1 + G(z)K(z)}, \tag{1}$$

with assuming the acoustic feedback path can be neglected ($F(z) \approx 0$) for the headphone applications. Then, the ideal feedforward controller for $E(z) \overset{!}{=} 0$ is given by $W_0(z) = \frac{P(z)}{G(z)}$. More details on the digital implementation of $W_0(z)$ is, e.g., given in [4] or [6]. This time-invariant approach offers compromised performance when the real $P(z)$ and $G(z)$ deviate from the nominal paths used in the design. The deviation is known as *uncertainty*. Therefore, time-variant methods which adapt to the current situation are getting increased interest in recent years. Feedback control requires more sophisticated methods, which explicitly consider the stability of the feedback loop in the presence of uncertainty about the acoustics of $G(z)$. One example is the $\mathscr{H}_\infty$-optimization as published in [7].

In general, all design methods require good knowledge about $P(z)$, $G(z)$ and $F(z)$. This includes the nominal

case, but also the uncertainty due to varying acoustic conditions. Especially for evaluating new algorithms it is crucial to have an accurate simulation of a real ANC system.

3 MEASUREMENT METHODS

For measurements of the secondary path $G(z)$ and the acoustic feedback $F(z)$, the inner loudspeaker is emitting an excitation signal $y(n)$. For the primary path $P(z)$ an external sound source $y_{\text{ext}}(n)$ is necessary, as $P(z)$ is the relative path between the inner and the outer microphone. Practically, two individual paths from the external speaker to the inner and outer microphone are measured: $Q_{\text{in}}(z)$ and $Q_{\text{out}}(z)$. They are later related to each other. An overview of all paths is given in Fig. 2. The acoustic component of each path is denoted by $*_A$.

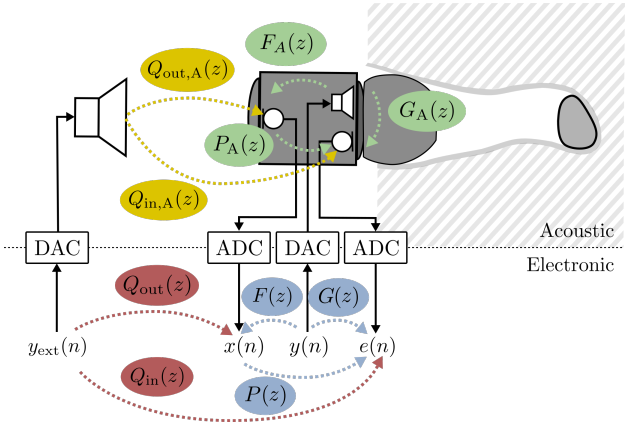

Figure 2. Transfer function components and measurement structure.

For the filter design, the primary path $P(z)$ is the transfer function between the digital outer disturbance and error signals, $x(n)$ and $e(n)$. It represents the passive attenuation of the headphone, however, is influenced by the microphone characteristics $H_{\text{mic,in}}(z)$ and $H_{\text{mic,out}}(z)$, yielding

$$P(z) = \frac{Q_{\text{in}}(z)}{Q_{\text{out}}(z)} = \frac{H_{\text{DAC}}(z)H_{\text{spk,ext}}(z)Q_{\text{in,A}}(z)H_{\text{mic,in}}(z)H_{\text{ADC}}(z)}{H_{\text{DAC}}(z)H_{\text{spk,ext}}(z)Q_{\text{out,A}}(z)H_{\text{mic,out}}(z)H_{\text{ADC}}(z)} = \frac{H_{\text{mic,in}}(z)}{H_{\text{mic,out}}(z)} \cdot \frac{Q_{\text{in,A}}(z)}{Q_{\text{out,A}}(z)} \tag{2}$$

$$= \frac{H_{\text{mic,in}}(z)}{H_{\text{mic,out}}(z)} \cdot P_{\text{A}}(z). \tag{3}$$

Thus, the primary path for the filter design $P(z)$ includes the acoustic component of the primary path $P_{\text{A}}(z)$ and the ratio between the two microphone characteristics, $H_{\text{mic,in}}(z)$ and $H_{\text{mic,out}}(z)$. The analog-to-digital (AD) and digital-to-analog (DA) converters are each assumed to have identical characteristics for all channels, $H_{\text{ADC}}(z)$ and $H_{\text{DAC}}(z)$.

The secondary path $G(z)$ is the transfer function between the control signal $y(n)$ and the error signal $e(n)$. It describes the influence of the control signal on the residual inside the ear canal, as

$$G(z) = H_{\text{DAC}}(z) \cdot H_{\text{spk}}(z) \cdot G_{\text{A}}(z) \cdot H_{\text{mic,in}}(z) \cdot H_{\text{ADC}}(z) \tag{4}$$

$$= H_{\text{EB}}(z) \cdot G_{\text{AF}}(z), \tag{5}$$

with the electronic backend $G_{\text{EB}}(z) = H_{\text{DAC}}(z) \cdot H_{\text{ADC}}(z)$ and the acoustic front-end $G_{\text{AF}}(z) = H_{\text{spk}}(z) \cdot G_{\text{A}}(z) \cdot H_{\text{mic,in}}(z)$. $H_{\text{ADC}}(z)$ and $H_{\text{DAC}}(z)$ contain the influence of the AD/DA converters as well as the necessary anti-aliasing filters.

The acoustic feedback path $F(z)$ is similarily defined as

$$F(z) = H_{\text{DAC}}(z) \cdot H_{\text{spk}}(z) \cdot F_{\text{A}}(z) \cdot H_{\text{mic,out}}(z) \cdot H_{\text{ADC}}(z) \tag{6}$$
$$= H_{\text{EB}}(z) \cdot F_{\text{AF}}(z). \tag{7}$$

It describes the leakage of the control signal to the outer microphone. The acoustic feedback needs to be considered for the design of a feedforward filter, when not sufficiently small due to bad design of the acoustic front-end.

3.1 Measurement Setups

The acoustic paths within this database were acquired in two different setups visualized in Fig. 3.

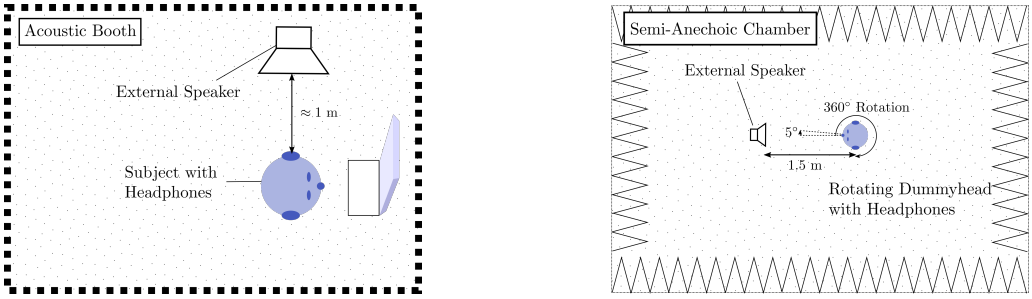

(a) In Acoustic Booth.

(b) In Semi-Anechoic Chamber.

Figure 3. The two measurement setups.

Acoustic Booth The first setup, is an acoustic booth used for listening tests (STUDIOBOX Premium). $P(z)$, $G(z)$ and $F(z)$ were measured during a listening test to evaluate the subjective performance of an active occlusion cancellation system [5]. The booth has an average attenuation from outside to inside of 44 dB. Its main purpose is to provide an acoustically isolated listening environment with a low reverberation time. It is not designed for free-field measurements and thus suffers from reflections visible in the primary paths later. However, the benefit of this dataset is the availibility of associated sets of $P(z)$, $G(z)$ and $F(z)$ for 23 persons (left and right side). Additionally, two handling cases were measured, including the situation *open* ("lying on the table") and *closed* ("closing the sound outlet"). Both were measured twice for both ears, resulting in four measurements of each case. The measurements were performed with a *dSPACE DS1005* real-time system with *DS2004* and *DS2102* AD/DA-extension boards. A reference measurement of this backend is part of the database, as described in Sec. 4.1. The sampling rate for the these measurements is $f_s = 48\,\text{kHz}$ and the impulse responses has 194400 samples measured with a 4.05 s long logarithmic sweep signal.

Semi-Anechoic Chamber Due to the large impact of reflections on the primary path measurements, a second dataset is included in this database. The second measurement set was originally acquired in a *semi-anechoic chamber* for an investigation of direction-of-arrival dependency of ANC systems [6]. The chamber has a concrete floor with a well-defined reflection. Apart from this floor reflection, it offers acoustic free field conditions above 100 Hz for acoustic measurements. The headphones were inserted into a Head Acoustics dummy head with integrated acoustic ear simulator (HMS II.3 with 6460 MFE VI amplifier, HEAD Acoustics GmbH, Herzogenrath, Germany). The headphone microphone signals were recorded with an RME soundcard to deduce $P(z)$. The database contains measurements for 72 different directions starting from a frontal position and with 5° resolution on horizontal plane. The sampling rate is $f_s = 48\,\text{kHz}$ and the impulse responses have 131072 samples measured with a 2.731 s long logarithmic sweep signal, each. In a separate step, but with the same fitting, $G(z)$ and $F(z)$

were acquired with the *dSPACE DS1005* real-time system. Here the impulse responses have 194400 samples measured with a 4.05 s long logarithmic sweep signal.

The external speaker for both cases was a Neumann KH120A (linear magnitude spectrum from 52 Hz to 21 kHz $\pm$ 3 dB). In both cases, the measurement system was placed outside the acoustic booth to minimize ambient noise.

3.2 Processing

The excitation signal was a logarithmic sweep. For the measurements in the semi-anechoic chamber as well as the post-processing the open source ITA Toolbox [2, 1] was used, which is developed at the Institute of Technical Acoustics, RWTH Aachen University. The database contains the unprocessed transfer functions, which only have been divided by the spectra of the excitation signals. For the visualization, the transfer function were postprocessed with a Hann window in the time domain. The cutoff times are indicated with the individual transfer functions in the later sections.

3.3 Tagging

The measurements are separated into *use cases* and *handling cases*, as the headphone might only require to provide performance while worn by the user. The use case measurements are additionally labeled based on the fitting of the headphone. The labels were chosen as *normal-fit*, *slightly-loose-fit* and *loose-fit* by observing the magnitude of the secondary paths at 90 Hz. The bounds were heuristically chosen to $[\infty, 0.8\,\text{dB}]$, $[0.8\,\text{dB}, -5\,\text{dB}]$ and $[-5\,\text{dB}, -\infty]$, based on the air leakage of the ear canal cavity. Handling cases include the situation *open* ("lying on the table") and *closed* ("closing the sound outlet").

4 MEASUREMENTS

In the following section, the measurements included in the database are visualized and described. All magnitude and phase responses were individually smoothed by 1/24th octave band smoothing filter for visualization.

4.1 Electronic Back-End

Fig. 4 shows the magnitude and phase the backend for three different configurations. The *dSPACE DS1005* real-time system with *DS2004* and *DS2102* extension boards by itself has a latency of 1 sample at 48 kHz (roughly 20.8 μs), shown as (- - -). The microphones require a DC bias voltage, which needs to be removed by a low-cut filter, visible by (·····). In our system it is realized as a digital first-order IIR filter. Also, the system uses succesive approximation register (SAR) converters, which require a dedicated analog anti-aliasing filter (AAF), shown by (- - -). The preamplification and the DC bias voltage for the microphones were provided by a RME Micstasy preamplifier (preamp), shown by (——). The system was used with the last configuration

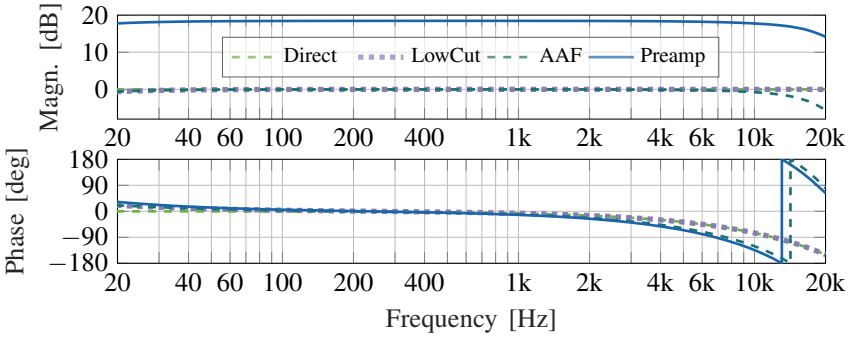

Figure 4. Measurements of the electronic backend.

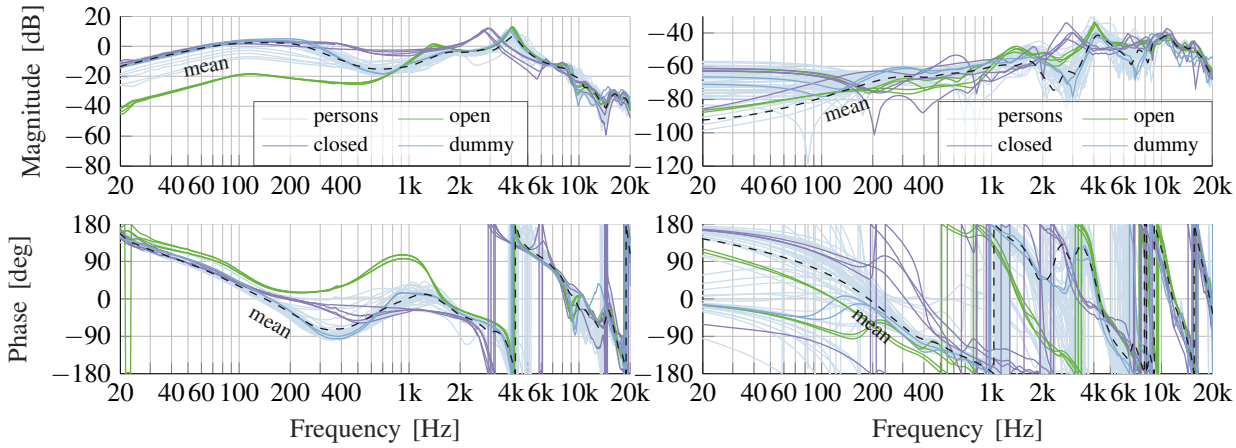

(a) Secondary Path $G(z)$.

(b) Acoustic Feedback Path $F(z)$.

Figure 5. Measurements of the secondary and acoustic feedback paths.

with low-cut, AAF and preamplifier. The complete system has a latency of roughly 37 μs, increasing towards low frequencies due to the low-cut. The reference measurements are provided to allow for correction of the electronic backend in the secondary and the acoustic feedback path. This can be realized by simple spectral division. The following transfer functions still contain the electronic backend and thus show $G(z)$ instead of $G_A(z)$ and $F(z)$ instead of $F_A(z)$.

4.2 Secondary Paths

The different secondary paths are shown in Fig. 5a. The impulse responses were processed with a one-sided Hann window starting after 150 ms and ending at 160 ms. From the acoustic booth measurements the different persons with various fittings (——) as well as the handling cases closed (——) and open (——) are shown. The complex mean (- - -) considers all these measurements. Additional to that, the dummy head measurements (——) from the setup in the semi-anechoic chamber are shown for comparison.

One can clearly see that the sound pressure provided by the speaker at low frequencies depends on the fitting. The larger the leakage of the headphone is, the less energy can be emitted at frequencies below 1 kHz. Directly closing the sound outlet of the headphone on the other hand allows for high energies at low frequencies. It also creates a resonance shift from 4 kHz to 3 kHz. This uncertainty in $G(z)$ poses a challenge for feedback and feedforward filter design.

4.3 Acoustic Feedback Paths

The different acoustic feedback paths are shown in Fig. 5b. The measurements were very noisy, as the acoustic feedback is relatively low in the Bose QC20. Higher sound pressure levels (SPL) of the excitation signal should be avoided to avoid harming the human subjects and avoiding to damage the speaker. Therefore, the impulse responses were processed with a very short one-sided Hann window starting after 4.5 ms and ending at 5 ms. Due to the short window size only frequencies above $f = 1/(5\,\text{ms}) = 200\,\text{Hz}$ contain relevant information.

4.4 Primary Paths

The primary path measurements are visualized in Fig. 6a for the acoustic booth and in Fig. 6b for the semi-anechoic chamber. The impulse responses were processed with a one-sided Hann window starting after 150 ms and ending at 160 ms. In general, both measurements show the expected low pass characteristic of $P(z)$ with varying cut-off frequency between 200 and 600 Hz for all but the open case. The open (——) and closed (——) case in Fig. 6a reveal that these cases need to be considered carefully, as they include a large amount of noise.

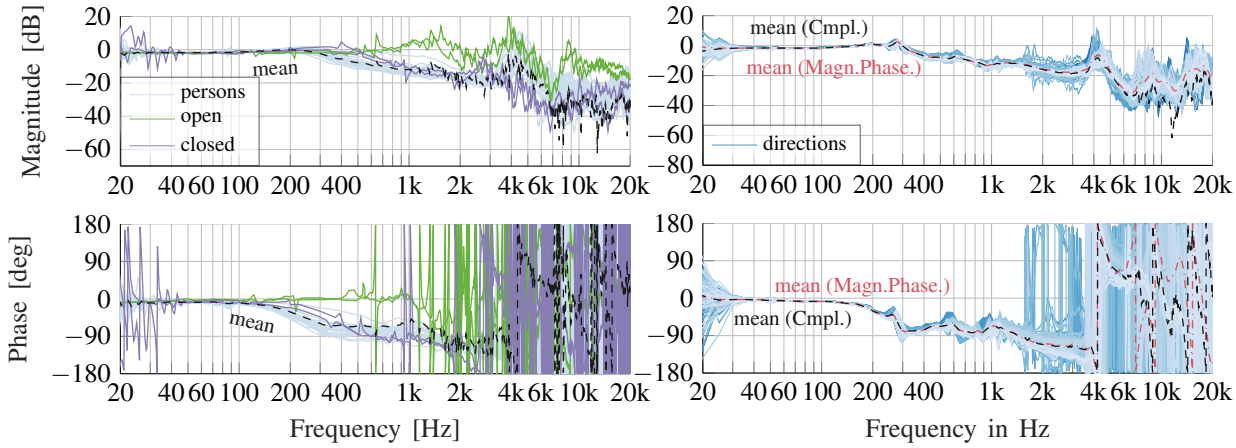

(a) Primary Path (Booth).

(b) Primary Path (Anechoic). 72 Directions.

Figure 6. Measurements of the primary paths.

Before being used, they might require additional smoothing.

Fig. 6b, also reveals one issue with the complex mean (- - -) value at high frequenices. When the phase is becoming very uncertain at high frequencies, the complex mean results in non-intuitive results [8]. One possible solution is to calculate a separate mean on magnitude and phase (-·-·-), which requires phase unwrapping. This is especially difficult in the presence of notches in the magnitude spectrum, which lead to discontinuities in the phase (e.g. Fig. 6a around 600 Hz for open (——)). A robust solution still needs to be proposed for this problem.

5 DATA FORMAT AND ACCESS

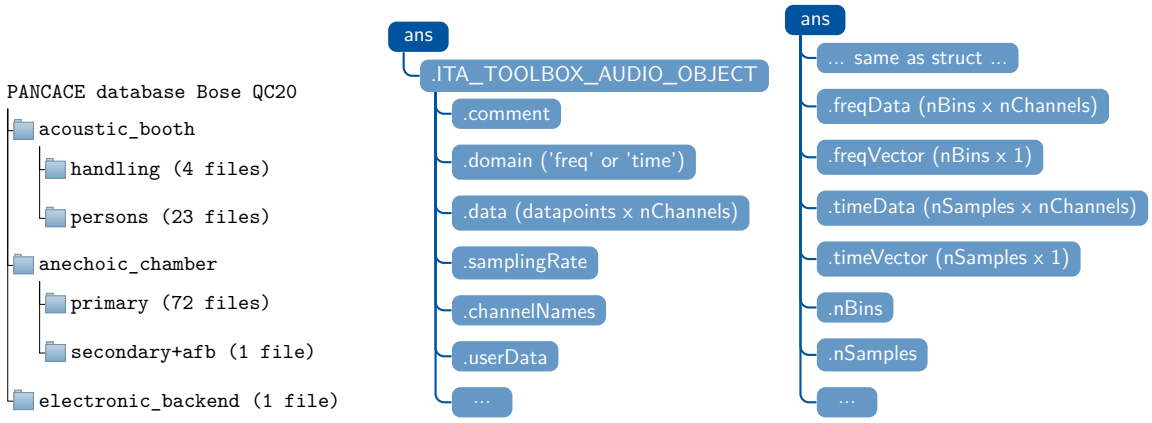

(a) Folder structure.

(b) Data struct (`ans=load(file,'-mat')`).

(c) ITA object (`ans=ita_read_ita(file)`)

Figure 7. Data structure.

Fig. 7 visualizes the structure of the database. On the left (Fig. 7a), the folder tree is shown, indicating where to find the different measurement files. The middle (Fig. 7b) gives a hint on the MATLAB struct, when loading the file via `load(file,'-mat')`. The file contains a MATLAB struct named `.ITA_TOOLBOX_AUDIO_OBJECT`. The data is accessible via `.data` and is represented either as real time domain data or as complex one-sided

frequency domain data, indicated by the `.domain` entry. It contains various additional metadata, including `.comment`, `.channelNames`, `.userData`, `.samplingRate`, etc. Without using the ITA toolbox, it is possible to extract the data, based on the `.data` and `.domain` entries. When using the native ITA toolbox command `ita_read_ita(file)`, this struct is directly converted into an itaAudio object. Some of the additional fields are shown in Fig. 7c. The ITA toolbox offers a more convient interface, e.g. by automatically transforming between time and frequency domain depending on the requested output. Furthermore, the ITA toolbox offers various powerful visualization and post-processing tools, including spectral inversion with regularization, time domain windowing, smoothing functions, system identification, etc.

6 CONCLUSIONS

This paper describes the iks | PANDAR database, which contains measured paths for filter design, system simulation and evaluation of ANC algorithms. It offers 46 primary, secondary and acoustic feedback path measurements from human subjects, 8 path measurements of handling cases, as well as primary path measurements for a dummy head for 72 different directions, with the associated secondary and acoustic feedback path. Reference measurements of the electronic backend are also included. The database is available for download under `http://iks.rwth-aachen.de/PANDAR/`.

ACKNOWLEDGEMENTS

The authors thank the Institute of Technical Acoustics (ITA), especially Jan-Gerrit Richter and Prof. Michael Vorländer, for their support during the measurements in the semi-anechoic chamber.

REFERENCES

[1] M. Berzborn, R. Bomhardt, J. Klein, J.-G. Richter, and M. Vorländer. The ITA-Toolbox : An Open Source MATLAB Toolbox for Acoustic Measurements and Signal Processing. In *Fortschritte der Akust. - DAGA 2017 43. Dtsch. Jahrestagung für Akust*, pages 222–225, 2017.

[2] P. Dietrich, M. Guski, M. Pollow, B. Masiero, M. Müller-Trapet, R. Scharrer, and M. Vorländer. ITA-Toolbox - An Open Source MATLAB Toolbox for Acousticians. In *DAGA 2012, 38. Jahrestagung für Akust. 19. - 22. März 2012 Darmstadt. Wiss / ed. Holger Hanselka*, pages 151–152. Deutsche Gesellschaft für Akustik e.V, 2012.

[3] S. Elliott. *Signal processing for active control*. Academic press, 2000.

[4] C. Hansen, S. Snyder, X. Qiu, L. Brooks, and D. Moreau. *Active control of noise and vibration*. CRC Press, 2012.

[5] S. Liebich, J. Fabry, P. Jax, and P. Vary. Active Occlusion Cancellation with Hear-Through Equalization for Headphones. In *2018 IEEE International Conference on Acoustics, Speech and Signal Processing (ICASSP)*, 2018.

[6] S. Liebich, J.-G. Richter, J. Fabry, C. Durand, J. Fels, and P. Jax. Direction-of-Arrival Dependency of Active Noise Cancellation Headphones. In *47th International Congress and Exposition on Noise Control Engineering (INTERNOISE)*, Washington, DC, USA, 2018. The Institute of Noise Control Engineering of the USA, Inc.

[7] S. Liebich, D. Rüschen, C. Anemüller, P. Vary, P. Jax, and S. Leonhardt. Active noise cancellation in headphones by digital robust feedback control. In *2016 24th European Signal Processing Conference (EUSIPCO)*, pages 1843–1847. Signal Processing Conference (EUSIPCO), 2016 24rd European, 2016.

[8] J. Panzer and L. Ferekidis. The use of continuous phase for interpolation, smoothing and forming mean values of complex frequency response curves. In *Audio Engineering Society Convention 116*, May 2004.